

Supplementary Information for Cycloaddition-dehydration continuous flow chemistry for renewable para-xylene production from 2,5-dimethylfuran and ethylene over phosphorous-decorated zeolite beta

Zhaoxing Wang,¹ Tejas Bimal Goculdas,^{1,2} Yung Wei Hsiao,¹ Wei Fan,^{2,3} and Dionisios G. Vlachos^{1,2}

¹Department of Chemical and Biomolecular Engineering, 151 Academy St., University of Delaware, Newark, DE 19716, USA

²Catalysis Center for Energy Innovation, Delaware Energy Institute (DEI), 221 Academy St., University of Delaware, Newark, DE 19716, USA

³Department of Chemical Engineering, University of Massachusetts, Amherst, MA 01003, USA

Corresponding author: vlachos@udel.edu

Analytical Product Quantification Data

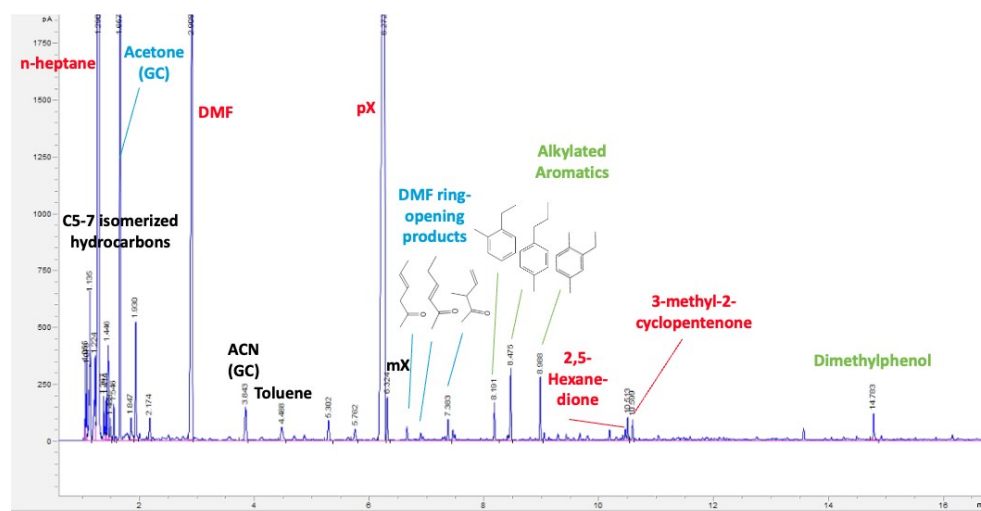


Figure S1. Typical gas chromatogram for the liquid product from P-BEA(25).

Furanic Carbon Balance for a Standard Reaction

Furanic Carbon balance of the reaction under typical reaction conditions (illustrated with the gas chromatogram above) was calculated for all identifiable, relevant species with nontrivial peaks. Note that the number of carbons used in the carbon balance calculation is typically 6 to reflect their DMF origin.

Table S1. Carbon balance of a standard reaction at 375 °C, 750 psig, 10 sccm ethylene flow, 0.025 mL/min liquid flow, 20 wt% DMF in feed (1.50 M in n-heptane). P-BEA (25) used

Species	Retention time, min	# Carbons used in carbon balance	Species Concentration in Product, M	Carbon balance, %	
DMF	2.908	6	0.390	25.92	
Toluene	4.488	6	0.0121	0.80	
pX	6.272	6	1.027	68.30	
mX	6.324	6	0.0189	1.26	
DMF Ring opening product 1	6.667	6	0.00705	0.47	
DMF Ring opening product 2	6.903	6	0.00376	0.25	
DMF Ring opening product 3	6.947	6	0.00236	0.16	
DMF Ring opening product 4	7.383	6	0.00983	0.65	
Alkylated intermediate 1	8.191	6	0.0173	1.15	
Alkylated intermediates 2	8.475	6	0.0337	2.24	
Alkylated intermediates 3	8.988	6	0.0275	1.83	
2,5-Hexanedione	10.472	6	0.00503	0.33	
Alkylated intermediates 4	10.513	6	0.0103	0.68	
Cyclopentenone	10.599	6	0.00800	0.64	
Dimethylphenol	14.783	6	0.0134	0.89	
Total			1.587	105.47	

Catalyst Benchmarking Data

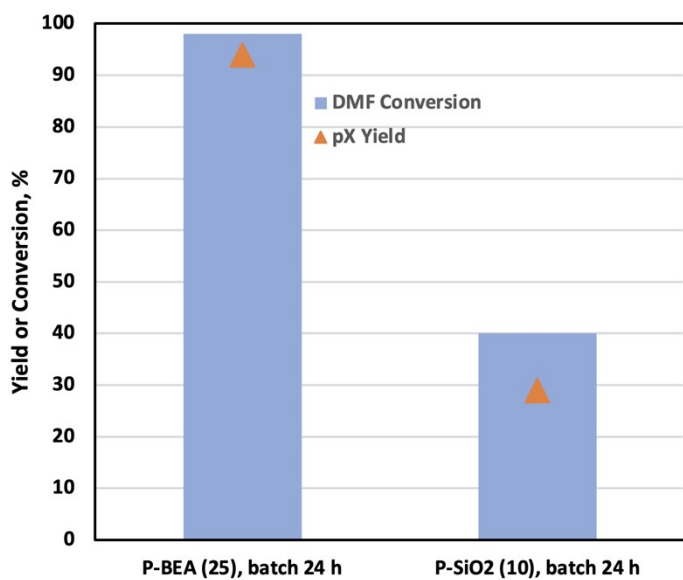


Figure S2. Catalyst performance of P-BEA(25) and P-SiO₂ (10 wt%, as reported in prior work¹) in batch, 24 h, magnetically stirred at 300 rpm, 62 bar headspace pressurization with ethylene, 250 °C, 1.35 M 2,5-dimethylfuran (DMF) in n-heptane as the solvent.

Catalyst Characterization Data

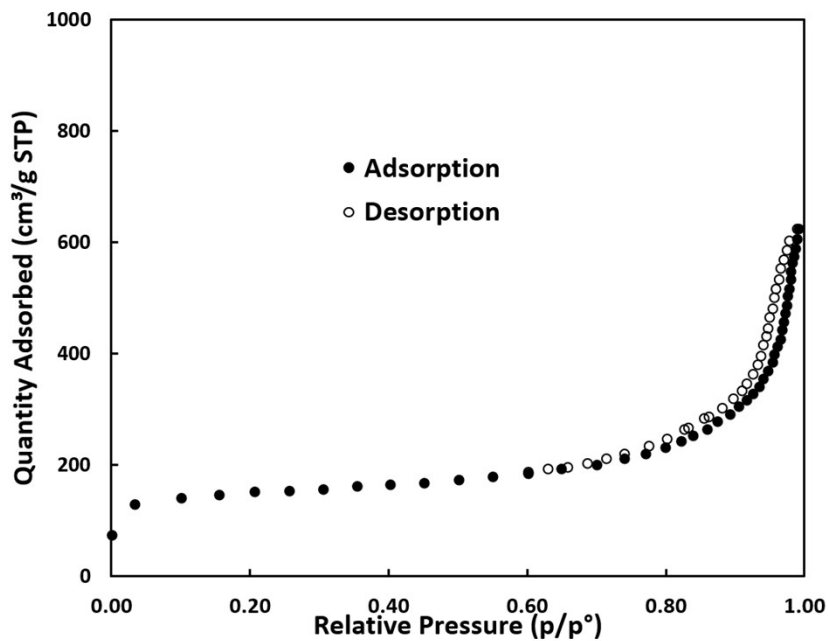


Figure S3. N₂ adsorption/desorption data of fresh P-BEA(25).

Table S2. Elemental analysis data of the catalysts used in this work, compared with literature data.^{2,3}

	BET Area, m²/g	Micropore volume using the t- plot method, cm³/g	Total pore volume from P/P₀=.97, H- K method cm³/g	ICP Si:P (mol)	Batch pX Yield @ 24h
P-BEA(25) this work	510	0.151	0.731	24.0	94%
P-BEA ³	-	-	-	23.9	-
P-BEA ²	499	0.1	0.801	27.1	97 %

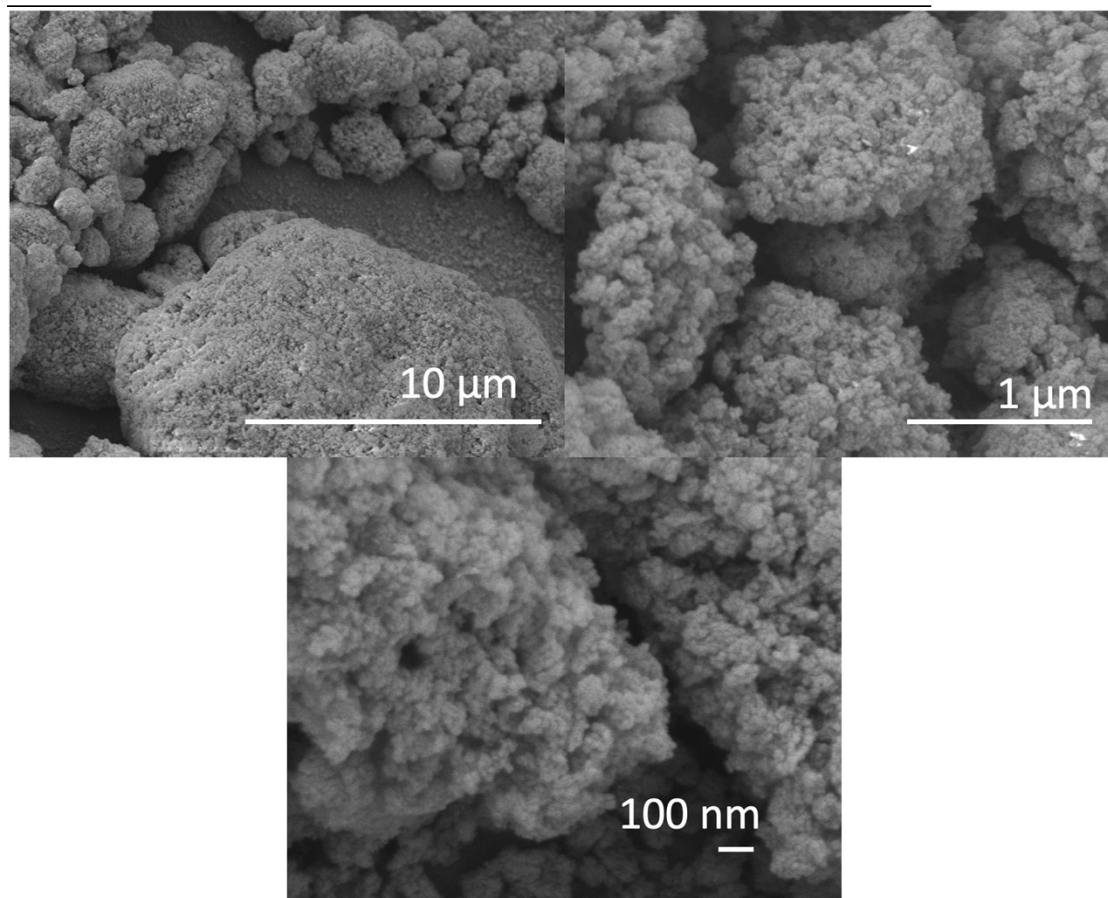


Figure S4. SEM images of unpelletized P-BEA(25).

Time-on-stream Data

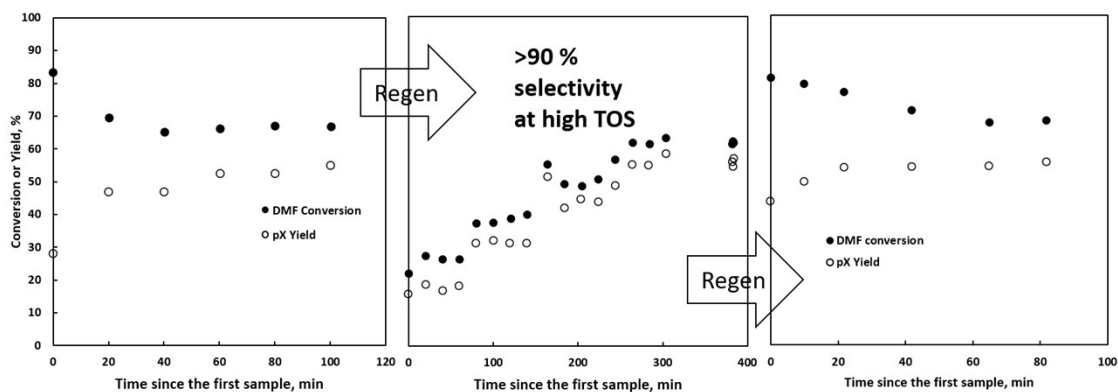


Figure S5. Performance vs. time on stream showing stabilization after ~1 h. Behavior during the P dependence experiments (center panel) after 5 h, with 550 °C in situ regeneration at 1 atm and 15 sccm air flow.

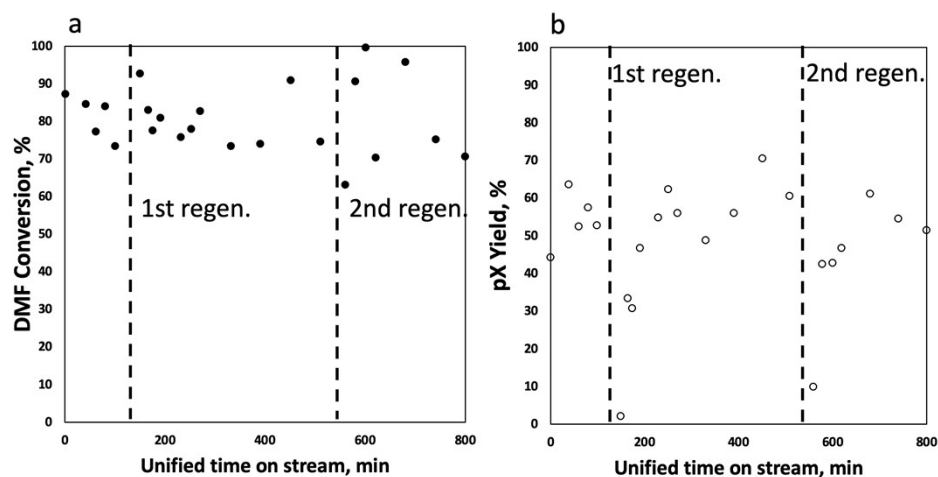


Figure S6. Time on stream performance of fresh P-BEA(25) and P-BEA(25) after up to 2 regeneration cycles, represented by a) DMF conversion and b) pX yield. Standard flow conditions: 375 °C, 750 psig, 20 wt% DMF in n-heptane, and 0.025 mL/min. In situ regeneration: reactor connected to air flow in a tube furnace at 15 sccm (routed through the column), 1 atm, 5 h at 550 °C with a 10 °C/min temperature ramp.

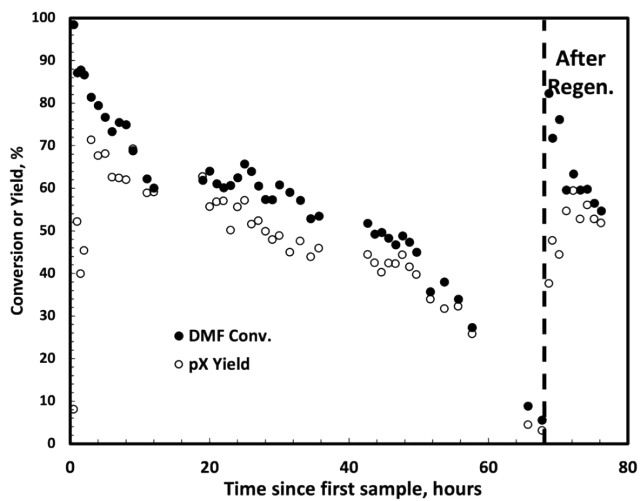


Figure S7. Extended time-on-stream performance of the reactor. Standard flow conditions: 375 °C, 750 psig, 20 wt% DMF in n-heptane, and 0.025 mL/min. *In situ* regeneration: reactor connected to air flow in a tube furnace at 15 scfm (routed through the column), 1 atm, 5 h at 550 °C with a 10 °C/min temperature ramp.

Supplementary Note 1: Thermodynamic Calculations

COSMO-RS Thermodynamic Predictions

Conductor-like solvation model for realistic solvation (COSMO-RS) using the Amsterdam Modeling Suite (AMS) implementation was used to predict the ternary vapor-liquid equilibrium (VLE) and the liquid-liquid equilibrium (LLE) of mixtures. COSMO-RS is an *ab initio/statistical mechanics* thermodynamic modeling tool for predicting phase behavior and partition coefficients used in our prior works.^{4,5} Screening charge density distributions of ethylene, para-xylene, and n-heptane are from the ADF-CRS2018 database. The screening charge density of DMF was calculated using the Amsterdam Density Functional with the default configurations for COSMO-RS screening charge calculations.

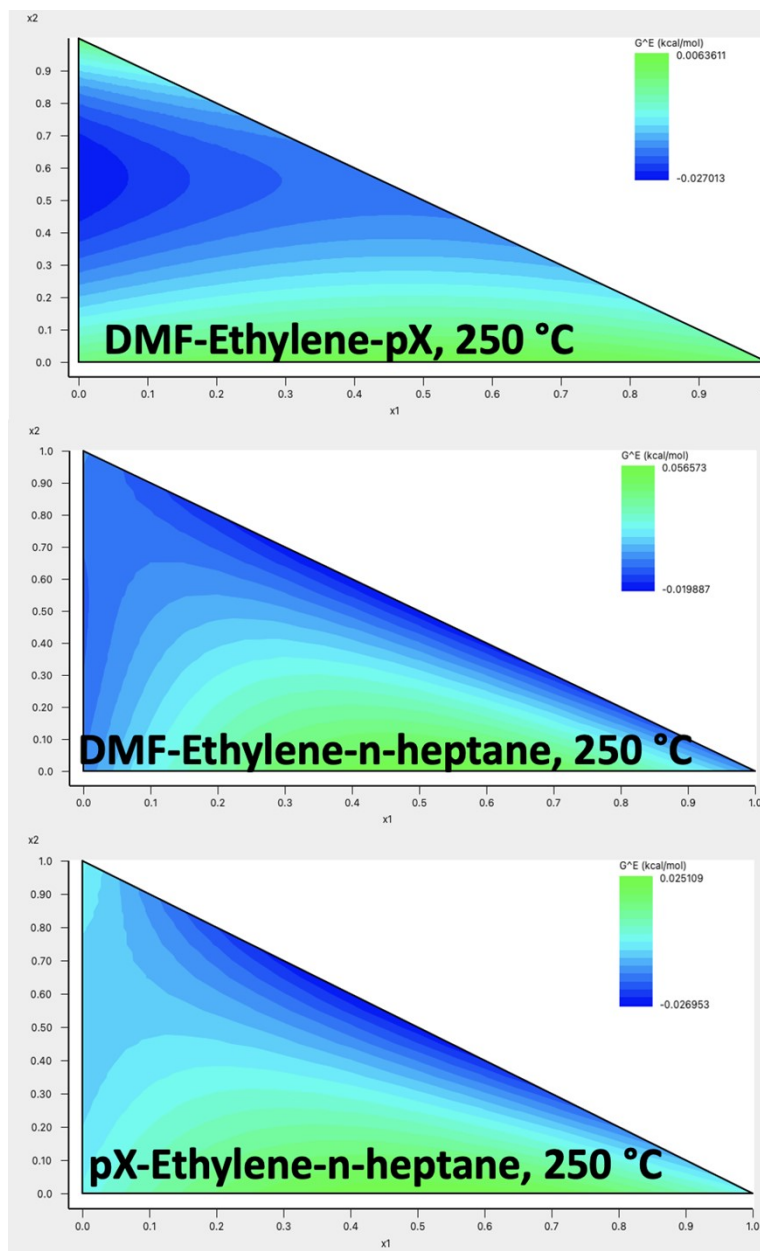


Figure S8. Example ternary diagram for vapor-liquid equilibrium (VLE) and liquid-liquid equilibrium (LLE) calculations for the DMF-ethylene-pX systems. All calculations above 250 °C predict a single phase for all ternary systems relevant to this work.

NRTL Thermodynamic Predictions in ASPEN Plus

ASPEN flowsheet simulations were used to predict the headspace properties and partitioning in batch and flow configurations investigated in this work. The flowsheet was created with separate heat exchangers, a mixer, and a flash drum to provide representative conditions.

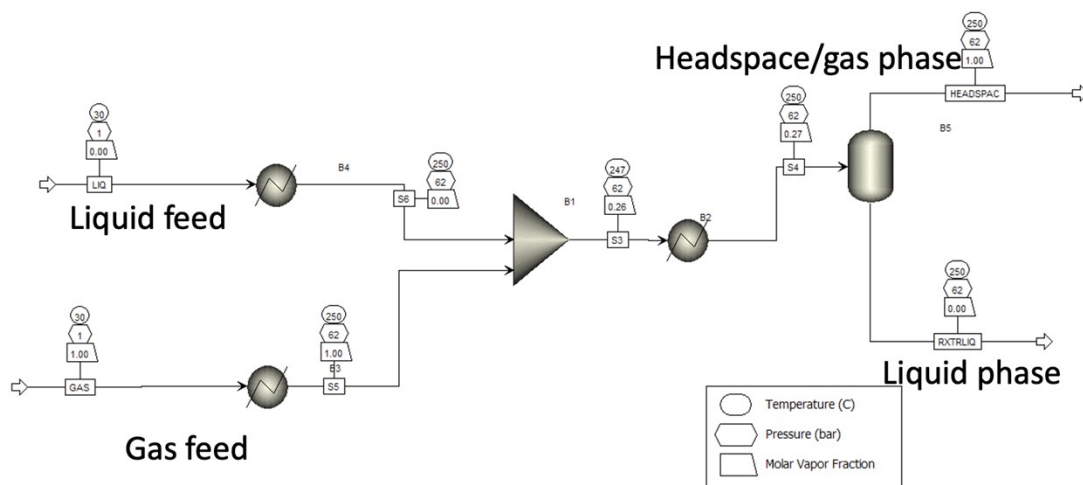


Figure S9. ASPEN Plus flowsheet for the thermodynamic phase behavior predictions. The NRTL model was used; the binary interaction parameters were obtained from the ASPEN database and regressed from literature data from NIST when available; UNIFAC was used when none was available (DMF-ethylene, DMF-pX, and DMF-heptane).

Component i	Component j	Source	Temp. Units	A ₁₁	A ₁₂	B ₁₁	B ₁₂	C ₁₁	D ₁₁	E ₁₁	F ₁₁	F ₁₂	TLOWER	TUPPER
P-XYL-01	N-HEP-01	APV120 VLE-IG	C	-1.01	0.519	532.182	-248.303	0.3	0	0	0	0	54.96	136.3
P-XYL-01	WATER	APV120 LLE-AS...	C	2.7734	162.477	296.665	-6046	0.2	0	0.1174	-23.4672	0	0	294.9
N-HEP-01	WATER	APV120 LLE-AS...	C	-9.8652	10.5468	-4795.66	-440.778	0.2	0	0	0	0	0	50
ETHYL-01	P-XYL-01	R-PCES	C	0	0	-596.253	963.962	0.3	0	0	0	0	25	25
ETHYL-01	WATER	USER	C	100	3.01946	527.78	783.123	0.3	0	0	0	0	25	25
ETHYL-01	25-D-01	R-PCES	C	0	0	-604.403	993.156	0.3	0	0	0	0	25	25
P-XYL-01	25-D-01	R-PCES	C	0	0	-106.447	82.0899	0.3	0	0	0	0	25	25
N-HEP-01	25-D-01	R-PCES	C	0	0	23.2121	28.7412	0.3	0	0	0	0	25	25
WATER	25-D-01	USER	C	-1.22825	1.29331	2602.79	949.762	0.3	0	0	0	0	25	25
ETHYL-01	N-HEP-01	USER	C	5.02708	-2.44897	0	0	0.3	0	0	0	0	-273.15	726.85

Figure S10. ASPEN Plus binary interaction parameters fit from NIST data and UNIFAC wherever indicated.

Table S3. ASPEN Plus thermodynamic predictions for batch phase at 250 °C, 62 bar, and 30 mL headspace. The nominal charged ethylene amounts were estimated based on ideal gas; also inflated to 1.12 x and 2.24 x to reflect ethylene absorption into the liquid and ethylene replenishment throughout the course of the reaction.

		Mole fraction trapped in headspace at equilibrium					
		Ethylene	n-heptane	DMF	pX	Water	All Species
Ethylene + heptane binary system	30 mL ethylene @ 62 bar	0.64	0.11	-	-	-	0.27
	Accounting for liquid phase absorption of ethylene, x1.12	0.69	0.14	-	-	-	0.32
	Accounting for liquid phase absorption of ethylene, x2.24	0.88	0.35	-	-	-	0.61
1.35 M DMF in liquid feed	30 mL ethylene @ 62 bar	0.57	0.10	0.10	-	-	0.24
	1.12 x	0.63	0.12	0.13	-	-	0.28
	2.24 x	0.86	0.32	0.34	-	-	0.58
1.35 M DMF all converted to pX and water	30 mL ethylene @ 62 bar	0.61	0.06	0.00	0.10	0.40	0.26
	1.12 x	0.65	0.07	0.00	0.12	0.45	0.30
	2.24 x	0.85	0.18	0.00	0.30	0.72	0.57

Table S4. ASPEN Plus flow reactor condition predictions.

Scenario	Ethylene sccm	Pred. Phases	Critical P, bar	Critical T, °C
Ethylene with n-heptane only	5	Single phase, "gas"	40.44	120.95
	10		44.06	80.53
	15		45.74	61.58
Ethylene and 20 wt% DMF in n-heptane	5	Single phase, "gas"	41.24	126.27
	10		44.50	84.64
	15		46.05	64.86
20 wt% DMF all converted to pX and water	5	Single phase, "gas"	56.06	152.44
	10		54.16	104.40
	15		53.22	80.49
40 wt% DMF	5	Single phase, "gas"	42.08	132.00
	10		44.98	89.22
	15		46.39	68.54
40 wt% DMF all converted to pX and water	5	Single phase, "gas"	69.95	180.61
	10		63.89	127.49
	15		60.70	99.51
Pure DMF	5	Single phase, "gas"	44.91	151.49
	10		46.69	105.46
	15		47.60	81.93
Pure DMF all converted to pX and water	5	Single phase, "gas"	103.53	248.70
	10		90.82	191.42
	15		83.02	156.25

All situations were predicted to be single-phase. Reaction mixture T and P setpoints are higher than the predicted critical points except in pX. The critical P is predicted above process P in these water-rich mixtures, indicating potential supercritical mixtures. It is unclear if the gas phase vs. supercritical phase is relevant when the external mass transfer is irrelevant. We do not expect supercritical state fluids to influence internal diffusion.

Thiele Modulus Analysis

The Thiele modulus h_T in this work was estimated using the equation specified by Hill and Root⁶:

$$h_T = \frac{V_p}{S_x} \times \sqrt{\frac{k''_1 S_g}{D_c V_g}} \quad (\text{Equation S1})$$

Here S_x is the exterior surface area of the catalyst pellet, V_p is the volume of the pellet, D_c is the diffusion coefficient of DMF into the catalyst particle, V_g is the void volume, S_g is the surface area and k''_1 is the measured rate constant. The parameter values are given in Table S4. S_x , V_p , V_g and S_g were calculated based on SEM and BET data, assuming the primary catalyst particles are uniform and spherical. The diffusivity of DMF was taken from Gancedo *et al.*⁷ We extracted the experimental rate constant from the work of Williams *et al.*, who conducted detailed kinetic experiments to measure the activation energy and rate constant for the Diels Alder reaction of propylene and DMF over an H-BEA catalyst.⁸ Compared to Williams *et al.*, the higher temperatures used in this work would increase the Thiele modulus due to the stronger temperature dependence of k .

The reaction system's Thiele modulus is estimated at 3.85 using the estimated parameters. This value is in the transition between a kinetically and internally diffusion-controlled regime. The uncertainty in the parameters does not allow for a more accurate assessment of diffusion limitations.

Table S5. Parameters used in the Thiele modulus estimation.

Radius (cm)	3.00E-06
Area (cm²)	1.13E-10
Volume (cm³)	1.13E-16
Void Volume (cm³/g)	0.73
S_g (cm²/g)	510.00
D_c (cm²/s)	2.0E-09
Rate Constant (s⁻¹)	42.3
Thiele Modulus	3.85

Mears Criterion

The Mears equation from Fogler is shown in Eq. 2.⁹ It is calculated using the observed reaction rate, bulk density, catalyst particle radius, reaction order, mass transfer coefficient, and bulk reactant concentrations. The variable values are given in the table below.

$$MR = \frac{-r'_A(\text{obs}) \times \rho_b \times R \times n}{k_c \times C_{Ab}} \quad \text{Equation (2)}$$

$$\rho_b = (1 - \text{porosity}) \times \rho_c \quad \text{Equation (3)}$$

Table S6. Parameters used to estimate the Mears criterion.

Variables	Definition	Original Values	Higher DMF Conc	Higher Cat Loading
MR	Mears criterion	0.28	0.1	0.1
$r'_A(\text{obs})$	Observed reaction rate	0.84 mol gcat ⁻¹ sec ⁻¹	0.84 mol gcat ⁻¹ sec ⁻¹	0.29 mol gcat ⁻¹ sec ⁻¹
ρ_b	Bulk density	1886.79 kg m ⁻³	1886.79 kg m ⁻³	1886.79 kg m ⁻³

ρ_c	Catalyst density	2400 kg m ⁻³	2400 kg m ⁻³	2400 kg m ⁻³
R	Catalyst particle radius	150 μm	150 μm	150 μm
n	Reaction order	1	1	1
k_c	Mass transfer coefficient	350 m sec ⁻¹	350 m sec ⁻¹	350 m sec ⁻¹
C_{Ab}	Bulk reactant concentrations	0.0024 mol liter ⁻¹	0.0068 mol liter ⁻¹	0.0068 mol liter ⁻¹

In the Diels-Alder cycloaddition of ethylene on DMF, DMF is the limiting reagent, and ethylene is in excess. Therefore, the reaction order was assumed to be one. The concentration of DMF was determined by considering the molar flow of DMF and the catalyst loading. To obtain an accurate measure, the concentration was adjusted for ethylene and heptane's total molar flow rate, as they impact the concentration of DMF in the catalyst bed. The observed reaction rate was calculated after 3 hours TOS to avoid the impact of catalyst deactivation. The catalyst density was assumed to be 2400 kg m⁻³, a typical zeolite value. The bulk density was calculated from the porosity of the bed using Equation 2. A catalyst bed depth of 0.0586 m was used at a loading of 0.5 g to estimate the void fraction. The mass transfer coefficient was assumed to be 350 m/s based on estimated values used for benzene hydrogenation in a trickle bed reactor¹⁰ and DMF hydrogenation¹¹.

An MR value above 0.15 indicates that the system is limited by external diffusion limitations. Using the estimated parameters, the Mears value was calculated to be 0.28, close to the threshold. This suggests a mild degree of external diffusion limitation, giving rise to the potential 1/WHSV dependence of the reaction system behavior.

The Mears criterion indicates that our system operates under external diffusion limitations. Increasing the DMF concentration to 4.67 M from 1.64 M and increasing its abundance at the catalyst surface could attain a Mears criterion of 0.1, assuming a constant observed reaction rate. Implementing this change while maintaining the same observed reaction rate would be challenging as we would also need to increase the system pressure to ~1500 psi to support the same phase composition. Similarly, varying the ethylene pressure would require the installation of a compressor, which is outside the experimental scope of a research laboratory. As an alternative, we could increase the catalyst loading to 1.42 g. This would decrease the WHSV by a factor of 2.9. As depicted in Figure 4, a lower WHSV results in a drop in selectivity, which is undesirable.

References

1. S. Liu, T. R. Josephson, A. Athaley, Q. P. Chen, A. Norton, M. Ierapetritou, J. I. Siepmann, B. Saha and D. G. Vlachos, *Sci Adv*, 2019, **5**, eaav5487.
2. H. J. Cho, L. Ren, V. Vattipalli, Y.-H. Yeh, N. Gould, B. Xu, R. J. Gorte, R. Lobo, P. J. Dauenhauer, M. Tsapatsis and W. Fan, *ChemCatChem*, 2017, **9**, 398-402.
3. J. Gulbinski, L. Ren, V. Vattipalli, H. Chen, J. Delaney, P. Bai, P. Dauenhauer, M. Tsapatsis, O. A. Abdelrahman and W. Fan, *Industrial & Engineering Chemistry Research*, 2020, **59**, 22049-22056.
4. Z. Wang, S. Bhattacharyya and D. G. Vlachos, *Green Chemistry*, 2020, **22**, 8699-8712.
5. Z. Wang, S. Bhattacharyya and D. G. Vlachos, *ACS Sustainable Chemistry & Engineering*, 2021, DOI: 10.1021/acssuschemeng.1c00982.
6. C. G. Hill and T. W. Root, *Introduction to Chemical Engineering Kinetics and Reactor Design*, Wiley, 2014.

7. J. Gancedo, L. Faba and S. Ordóñez, *ACS Sustainable Chemistry & Engineering*, 2022, DOI: 10.1021/acssuschemeng.2c02285.
8. C. L. Williams, K. P. Vinter, C.-C. Chang, R. Xiong, S. K. Green, S. I. Sandler, D. G. Vlachos, W. Fan and P. J. Dauenhauer, *Catalysis Science & Technology*, 2016, **6**, 178-187.
9. H. S. Fogler, *Elements of Chemical Reaction Engineering*, Pearson, 2006.
10. K. C. Metaxas and N. G. Papayannakos, *Industrial & Engineering Chemistry Research*, 2006, **45**, 7110-7119.
11. H. Goto, A. Takagaki, R. Kikuchi and S. T. Oyama, *Applied Catalysis A: General*, 2017, **548**, 122-127.